Journal of Adhesion Science and Technology

ISSN: 0169-4243 (Print) 1568-5616 (Online) Journal homepage: http://www.tandfonline.com/loi/tast20

Investigation on the inhibition effect of aspartic acid and Zn^{2+} ions on carbon steel surface in aqueous solution

M. Prabakaran, S. Ramesh & V. Periasamy

To cite this article: M. Prabakaran, S. Ramesh & V. Periasamy (2015): Investigation on the inhibition effect of aspartic acid and Zn^{2+} ions on carbon steel surface in aqueous solution, Journal of Adhesion Science and Technology, DOI: 10.1080/01694243.2015.1087754

To link to this article: http://dx.doi.org/10.1080/01694243.2015.1087754

JOURNAL OF ADHESION SCIENCE AND TECHNOLOGY, 2015
http://dx.doi.org/10.1080/01694243.2015.1087754

Taylor & Francis
Taylor & Francis Group

Investigation on the inhibition effect of aspartic acid and Zn^{2+} ions on carbon steel surface in aqueous solution

M. Prabakaran[a], S. Ramesh[b] and V. Periasamy[b]

[a]Department of Chemistry, Gnanamani College of Technology, Namakkal, Tamil Nadu, India; [b]Department of Chemistry, The Gandhigram Rural Institute-Deemed University, Gandhigram 624302, Tamil Nadu, India

ABSTRACT

A protective film has been formed on the surface of carbon steel in aqueous environment using a synergistic mixture of an environment-friendly inhibitor, aspartic acid, and Zn^{2+}. The synergistic effect of aspartic acid (AS) in controlling corrosion of carbon steel has been investigated by gravimetric studies in the presence of Zn^{2+}. The formulation consisting of AS and Zn^{2+} has an excellent inhibition efficiency. The results of potentiodynamic polarization revealed that the formulations are of mixed-type inhibitor. Impedance studies of the metal/solution interface indicated that the surface film is highly protective against the corrosion of carbon steel in the aqueous environment. X-ray photoelectron spectroscopic analysis of the protective film showed the presence of the elements iron, nitrogen, oxygen, carbon, and zinc. The spectra of these elements in the surface film showed the presence of oxides/hydroxides of iron(III), $Zn(OH)_2$, and [Fe(III)/Fe(II)–Zn(II)-AS] complex. Further, surface characterization techniques such as Fourier transform infrared spectroscopy, scanning electron microscopy, and atomic force microscopy are used to ascertain the nature of the protective film formed on the carbon steel surface.

ARTICLE HISTORY
Received 26 March 2015
Revised 24 August 2015
Accepted 25 August 2015

KEYWORDS
Corrosion; carbon steel; aspartic acid; polarization; XPS; AFM

1. Introduction

Carbon steel is the primary building material for industrial cooling water systems.[1] Corrosion of carbon steel is one of the major challenges in such systems. Corrosion is the deterioration of materials by chemical interaction with their environment. The corrosion in cooling water systems deeply affects the health of human being and economic level of the world. The use of inhibitors is one of the most economical and convenient methods of reducing corrosive attack on metals.[2,3] The inhibitors are tremendously effective even in very small concentrations and efficiently reduce the corrosion rate. The use of organic molecules as corrosion inhibitor is one of the most practical methods for protecting against the corrosion and it is becoming increasingly popular.[4] Commonly, organic molecules containing nitrogen, sulfur, oxygen, phosphorus, and aromatic rings or multiple attachments in their

CONTACT S. Ramesh ✉ drsramesh_56@yahoo.com

molecular structure have been accounted to be efficient inhibitors.[5–7] These compounds get adsorbed onto the surface of metal from the bulk of environment, forming a protective film on the metal surface.[8] The inhibition efficiency increases in the order $O < N < S < P$.[9] This trend is probably linked to the disposition of an atom to donate electrons and is hence related to the electronegativity of the atom. Oxygen has the highest electronegativity value (3.44) and thus it receives the least propensity to donate electrons while phosphorus has the least electronegativity value (2.19) and has the highest tendency to donate electrons. The common corrosion inhibitors such as chromates,[10] nitrites,[11] and aromatic heterocyclic compounds [12] are environmentally hazardous. The replacement of these inhibitors with new environment-friendly materials is essential. Amino acids are naturally occurring, non-toxic, biodegradable, relatively inexpensive, and completely soluble in aqueous media. Amino acids were reported as good corrosion inhibitors for many metals in different aggressive media.[13–17] The environment-friendly aspartic acid is chosen as the corrosion inhibitor for this present work. Aspartic acid (AS) used as a corrosion inhibitor for brass in aqueous sodium chloride solution has been reported in the literature [18]. Kolata and Silverman [19] showed the corrosion inhibition of steel by aspartic acid. Also aspartic acid has been reported as a corrosion inhibitor for brass,[18] copper,[20] aluminum,[21], and cobalt.[22] Synergism has become an increasingly important phenomenon and serves as the basis for most modern corrosion inhibiting formulations. Synergistic effect existing among amino acid and Zn^{2+} on the corrosion inhibition of metals has been studied in the literature[18]. So, the synergistic effect of Zn^{2+} ions on the capability of amino acid has also been examined in order to ascertain the specific manner in which the compound exerts its inhibiting action.

In the present work, the inhibitive effect with a new organic inhibitor viz. AS and Zn^{2+} ions in controlling the corrosion of carbon steel in neutral aqueous environment containing low chloride has been studied by the gravimetric studies. The corrosion inhibition was further investigated by means of electrochemical studies, viz. potentiodynamic polarization and electrochemical impedance spectroscopy (EIS). Surface characterization studies, viz. X-ray photoelectron spectroscopy (XPS), Fourier transform infrared spectroscopy (FTIR), scanning electron microscopy (SEM) and atomic force microscopy (AFM) were used to examine the nature of protective film formed on the metal surface. A plausible mechanism of corrosion inhibition is proposed.

2. Experimental

2.1. Materials

In all the studies, the specimens were chosen from a single sheet of carbon steel with the following composition: 0.026% S, 0.035% P, 0.58% Mn, 0.104% C and the rest iron. For gravimetric measurements and FTIR, the specimens with dimensions of 3.5 cm × 1.5 cm × 0.2 cm, were polished to a mirror finish with 1/0, 2/0, 3/0, 4/0, 5/0, and 6/0 emery polishing papers, respectively, degreased with acetone, and dried. The dimensions of the specimens are 1.0 cm × 1.0 cm, and 0.2-cm thickness of the electrode was encapsulated by araldite paste and the effective exposed surface area is 1 cm^2 was used for electrochemical studies. Specimens with dimensions 1.0 cm × 1.0 cm × 0.2 cm were used for surface examination studies.

The molecular structure of AS is shown in Figure 1. The tested compound, namely AS purchased from Sigma-Aldrich was used without further purification. Zinc sulfate ($ZnSO_4{\cdot}7H_2O$), sodium chloride, and other reagents were analytical grade chemicals. All

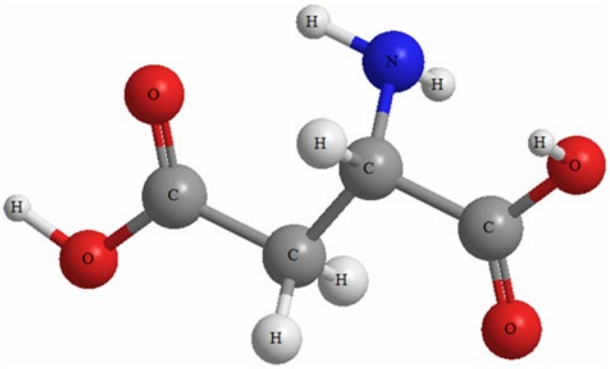

Figure 1. Molecular structure of AS.

the solutions were prepared using triple distilled water. For all these studies, an aqueous solution of 60 ppm chloride has been chosen as control because the water used in cooling water systems is generally either demineralized water or unpolluted surface water

2.2. Gravimetric studies

The carbon steel specimens of volume 3.5 cm × 1.5 cm × 0.2 cm were abraded consecutively with different grades of emery papers (1/0, 2/0, 3/0, 4/0, 5/0, and 6/0) washed with triple distilled water, cleaned with acetone, dried, and kept in moisture-free desiccator. After being weighed accurately by a Mettler balance, AE 240 model with high sensitivity, the specimens were immersed in control solution with and without various concentrations of the inhibitor formulations at room temperature. After 7 days of immersion, the specimens were taken out, rinsed thoroughly with triple distilled water, dried, and weighed accurately again. Experiments were carried out in triplicate. The average weight loss ΔW (mg) was calculated using the following equation:

$$\Delta W = W_1 - W_2 \tag{1}$$

where W_1 and W_2 are the average weight of specimens before and after immersion, respectively.

2.3. Inductively coupled plasma-optical emission spectroscopy (ICP-OES)

Inductively coupled plasma-optical emission spectrometer was used to analyze the gravimetric solutions. The collected gravimetric solutions were analyzed for the presence of Fe, Zn, and P in the test solution after the immersion of carbon steel in the control and inhibitor solution for seven days using Optima 5300 DV, Perkin Elmer.

2.4. Electrochemical studies

The electrochemical experiments, viz. potentiodynamic polarization and electrochemical impedance spectroscopy, were performed using CHI Electrochemical analyzer model 760D and the experimental data were analyzed by the use of EC-Lab software. The analyzer had a three-electrode cell setup having a carbon steel working electrode (WE) embedded in a Teflon holder with exposed surface area of 1.0 cm^2 in corrosive environment, a saturated calomel electrode (SCE) as reference electrode, and a platinum wire as counter electrode (CE). The reference electrode was placed close to the working electrode to minimize IR contribution. The working electrode was first immersed in the test solution for 1 h to establish a steady-state open circuit potential (E_{ocp}). After measuring the open circuit potential, potentiodynamic polarization curves were obtained with a scan rate of 1 mV/s in the potential range between ± 200 mV relative to the E_{ocp}. Corrosion current density values were obtained by the Tafel extrapolation method at points 50 mV more positive and more negative than the corrosion potential (E_{corr}). From the Tafel extrapolation method, other electrochemical parameters such as corrosion potential, anodic Tafel slope, and cathodic Tafel slope were also obtained. The inhibition efficiencies (IE_p) were calculated from I_{corr} values using the following relation:

$$\text{IE}_\text{p}(\%) = \left[\frac{I\text{corr} - I'\text{corr}}{I\text{corr}}\right] \times 100 \tag{2}$$

where I_{corr} and I'_{corr} are the corrosion current densities in the case of control and inhibitor solutions, respectively.

EIS experiments were performed at a potential open circuit in the frequency range from 100 kHz to 80 mHz, with a signal amplitude perturbation of 5 mV. The electrochemical impedance parameters such as charge transfer resistance (R_{ct}), constant phase element (CPE), and CPE exponent (n) were obtained from Nyquist plots. The inhibition efficiencies (IE_i) were calculated using the following equation:

$$\text{IE}_\text{I}(\%) = \left[\frac{R'_{ct} - R_{\text{ct}}}{R'_{\text{ct}}}\right] \times 100 \tag{3}$$

where R_{ct} and R'_{ct} are the charge transfer resistance values in the absence and presence of the inhibitor, respectively.

2.5. Surface examination studies

The nature of the protective film formed on the surface of the carbon steel specimen was characterized by XPS, FTIR, SEM, and AFM.

2.5.1. X-ray photoelectron spectroscopy

XPS measurements of the protective films were performed an AXIS 165 from the Kratos analytical photoelectron spectrometer. The carbon steel specimens were irradiated with the monochromated Al Kα X-ray source ($h\nu = 1486.6$ eV) operated at 100 W. The spectra were recorded at an electron take-off angle of $\theta = 90^\circ$. Deconvolution spectra were recorded with an analyzer pass energy of 80 eV, with a step of 0.1 eV for the elements of interest namely Fe 2p, O 1s, C 1s, N 1s and Zn 2p. Binding energies for the deconvolution spectra were corrected individually for each measurement set, based on a value of 285.0 eV for the C–C component of C 1s.

Table 1. Corrosion rate (mdd) and inhibition efficiencies (%) of carbon steel in the absence and presence of inhibitor system (AS–Zn^{2+}) obtained by gravimetric studies.

	Zn^{2+} (ppm)															
	0		10		20		50		75		100		125		150	
AS (ppm)	CR	IE	CR	IE	CR	IE	CR	IE	CR	IE	CR	IE	CR	IE	CR	IE
0																
10			9.54	28	2.53	81	1.90	86	8.18	38	6.33	52	8.08	39	7.48	44
25			8.84	34	1.37	90	2.72	80	8.21	38	7.12	46	5.71	57	5.23	61
50			9.20	31	1.57	88	0.94	93	6.27	53	5.41	59	6.59	50	5.64	58
75			9.92	25	1.66	88	1.46	89	3.13	76	4.82	64	5.01	62	5.74	57
100			8.99	32	1.24	91	**0.52**	**96**	2.07	84	2.10	84	2.17	84	5.16	61
150			8.220	38	0.93	93	0.72	95	4.37	67	3.92	71	1.56	88	7.32	45
200			7.78	41	1.64	88	0.62	95	5.29	60	4.65	65	2.07	84	8.22	38
250			8.65	35	1.35	90	0.72	95	6.49	51	6.57	51	1.34	90	6.26	53

Note: Bold values indicate the higher inhibition efficiency.

2.5.2. FTIR spectra

FTIR spectra were recorded with a frequency ranging from 4000 to 400 cm^{-1} with a resolution of 4 cm^{-1}. The FTIR spectra of pure AS and the protective film were recorded by the use of the KBr pellet method using JASCO 460 plus model instrument.

2.5.3. Scanning electron microscopy

The polished carbon steel specimens were immersed in solutions containing 60 ppm chloride ions in the absence and in the presence of the inhibitor formulation. After 7 days, the carbon steel specimens were taken out, washed with triple distilled water and dried. The SEM photographs of the surfaces of the carbon steel specimens were obtained using a VEGA3 TESCAN model scanning electron microscope with a resolution of 3.5 nm.

2.5.4. Atomic force microscopy

The protective films were examined with AFM images using NTEGRA PRIMA–NTMDT, Ireland. AFM topographical images of the entire samples for a scanned area of 10 × 10 μm. The three- and two-dimensional topography of surface films gave various roughness parameters of the protective film i.e., root mean square (RMS) value.

3. Results and discussion

3.1. Gravimetric measurements

In general, the efficiency of an organic substance as an inhibitor for metallic corrosion depends on the structure and the concentration of the inhibitor, the nature of the metal, and the other experimental conditions.[19] The corrosion rate CR (mgdm^{-2} days^{-1}) and the values of inhibition efficiency IE_g (%) obtained from gravimetric measurements of carbon steel after 7 days of immersion in control solution containing 60 ppm chloride ions with and without the addition of various concentrations of the inhibitor formulations is shown in Table 1. The values of CR and IE_g were calculated using the following equations

$$CR(\text{mdd}) = \left[\frac{\Delta W}{St}\right] \times 100 \tag{4}$$

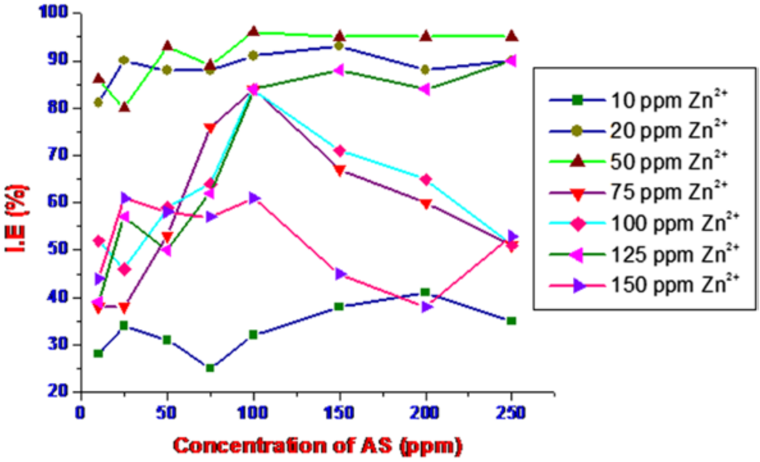

Figure 2. Inhibition efficiency as a function of the concentration of AS.

$$\mathrm{IE_g}(\%) = \left[\frac{CR_0 - CR_\mathrm{I}}{CR_0}\right] \times 100 \tag{5}$$

where ΔW (mg) is the weight loss, S (dm^2) is the surface area, t (days) is the immersion period, CR_0 and CR_I are corrosion rates in the absence and the presence of inhibitor, respectively.

The carbon steel was immersed in control solution in the absence and presence of various concentrations of the AS (10–250 ppm) and Zn^{2+} (10–150 ppm). The results of the gravimetric studies using the inhibitor system AS–Zn^{2+} at various concentrations of both constituents are shown in Figure 2. Initially, carbon steel corroded in control solution and showed a very high corrosion rate with the heavy metal loss. The corrosion rate decreased and the inhibition efficiency increased appreciably by the addition of 50 ppm Zn^{2+} and 100 ppm AS and the efficiency reached up to 96%. It is evident from gravimetric result that AS by itself is a poor corrosion inhibitor. Addition of Zn^{2+} ions to control solution accelerated the corrosion of carbon steel and the maximum acceleration was observed at 150 ppm Zn^{2+} ion concentration. However, a combination of AS and Zn^{2+} ion exhibited interesting behavior. In the combination consisting of 10 ppm Zn^{2+} ions and AS 10–250 ppm, corrosion inhibition was observed. The formulation consisting of 10 ppm Zn^{2+} and 100 ppm AS shows an inhibition efficiency of 32%. But, with increasing concentration of AS, keeping Zn^{2+} ions at 10 ppm, the inhibition efficiency was found to decrease. A similar trend was observed even in the other concentrations of Zn^{2+} ions, viz. 20–150 ppm. On increasing the concentration of Zn^{2+} from 10 to 20 ppm, the inhibition efficiency of 91% was obtained at 100 ppm AS. Increasing the concentration of Zn^{2+} ions, keeping AS at 100 ppm, the inhibition efficiency was found to increase. With the increasing concentration of AS beyond 100 ppm, the inhibition efficiency decreased. The combination containing 50 ppm Zn^{2+} and 100 ppm AS has achieved high inhibition efficiency (IE) of 96%. In this way, a synergistic corrosion inhibition effect is noticed. After this concentration, no appreciable change in efficiency was observed. It can be interpreted that low concentrations of Zn^{2+} are insufficient to form

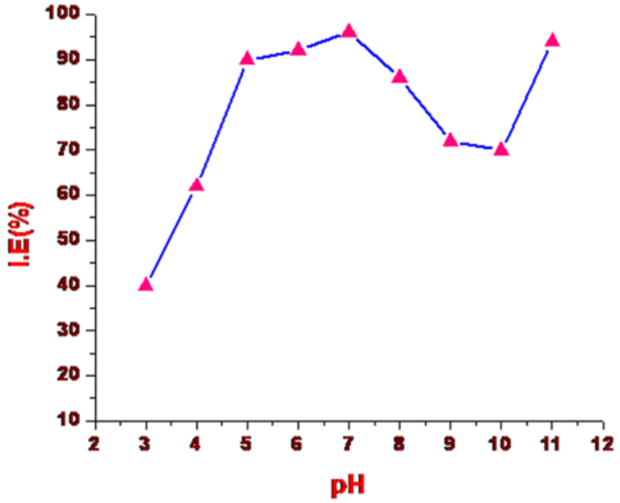

Figure 3. Effect of pH.

a protective film with AS on the carbon steel surface. At lower concentrations of Zn^{2+}, the AS is precipitated as AS–Zn^{2+} complex in the bulk of the solution. AS is not transported towards the carbon steel surface. Only on increasing concentrations of Zn^{2+} from 50 ppm to 150 ppm, the maximum efficiency 90% is obtained. A thin multicolored protective surface film is observed on the surface of the carbon steel during the gravimetric studies. The synergistic combination of 50 ppm Zn^{2+} and 100 ppm AS offered the maximum inhibition efficiency of 96%. The anodic reaction is controlled by the formation of Fe^{2+}–AS complex at the sites on the carbon steel surface. The cathodic reaction is controlled by the formation of $Zn(OH)_2$ on the cathodic sites on the carbon steel surface.

3.2. Effect of pH

The inhibitor system containing AS (100 ppm) and Zn^{2+} (50 ppm) was selected for further studies at the pH range of 3–11 because of its good inhibition efficiency. The effect of pH on the corrosion inhibition efficiency of 100 ppm AS and 50 ppm Zn^{2+} ions is shown in Figure 3. It is evident from the results obtained that the inhibition efficiency decreases on increasing the pH from 7.0 to 9.0 in alkaline medium and also on decreasing the pH from 5.0 to 3.0. The highest inhibition efficiency could be obtained in the pH range 5.0–7.0. However, interestingly, the corrosion inhibition efficiency again increases from pH 10.0 to 11.0. This is due to formation of sodium zincate over the metal surface, protecting the metal due to passivation. This inhibitor formulation is effective in the pH range 5.0–7.0 and also at pH 11.0.

3.3. Inductively coupled plasma-optical emission spectroscopy

The solution containing 60 ppm chloride, 100 ppm AS, and 50 ppm Zn^{2+} ions in which carbon steel specimens were immersed for 7 days was analyzed for Fe and Zn^{2+} by ICP-OES. Inspection of obtained results, given in Table 2, clearly shows that the concentration of iron

Table 2. The analysis results of the solution immersion by ICP-OES.

Sample	Fe (ppm)	IE $(M_i - M_f)/M_i$ %		Zn (ppm)
Control solution	$M_i = 40.00$	–	Before immersion of metal specimen	50.00
AS–Zn^{2+}	$M_f = 2.20$	95	After immersion of metal specimen for 7 days	4.20

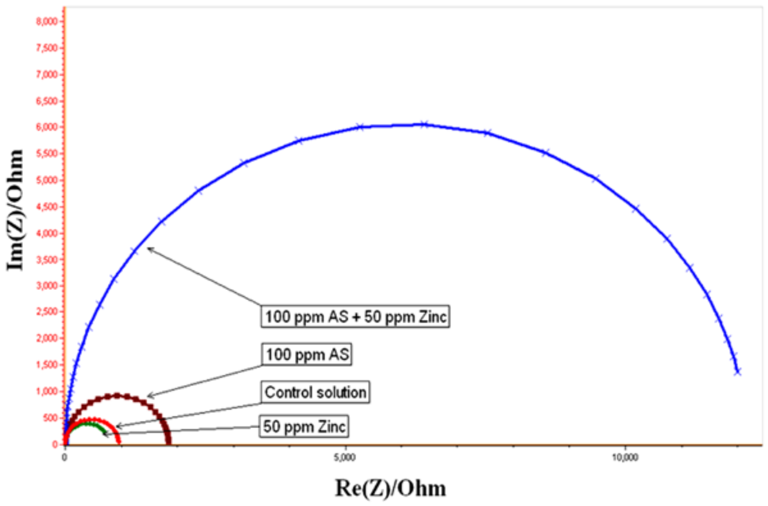

Figure 4. Nyquist plots for carbon steel immersed in different test solutions.

Table 3. Tafel parameters obtained from potentiodynamic polarization studies of carbon steel immersed in the absence and in the presence of inhibitor system.

Concentration (ppm)		Tafel parameters				
AS	Zn^{2+}	E_{corr} (mV/SCE)	I_{corr} (μA/cm^2)	β_a (mV/decade)	β_c (mV/decade)	IE_p (%)
–	–	−487.62	22.68	209	212	–
–	50	−633.83	23.30	208	209	–
100	–	−557.60	13.55	235	187	40
100	50	−578.01	1.57	157	148	93

in the solution without inhibitor was very high, the presence of the inhibitor solution limited the passage of the iron in solution. Indeed, the obtained value of inhibition efficiency is in good agreement with that obtained using gravimetric measurements. The results show that out of 50 ppm Zn^{2+} ions, 45.80 ppm Zn^{2+} ions have diffused from the bulk of the solution and adsorbed on the metal surface. The results show that an appreciable amount of Zn^{2+} ions has diffused from the bulk of the solution to the metal surface and incorporated in the protective film.

3.4. *Electrochemical impedance spectroscopy*

Impedance method provides information about the kinetics of the electrode process and simultaneously about the surface properties of the investigated systems. Mechanistic information about the reaction at the surface can be explained from the shape of the Nyquist

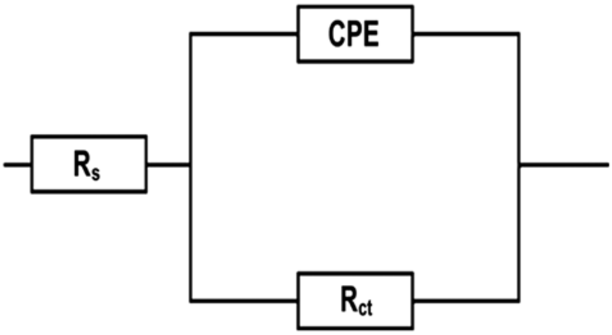

Figure 5. Equivalent electrical circuit used to fit the Nyquist plots.

plots. This method is most widely used to study the corrosion inhibition process.[20] Nyquist plots of carbon steel in control solution with and without inhibitor formulations are presented in Figure 4. The charge transfer resistance (R_{ct}) and double layer capacitance (C_{dl}) were the parameters obtained from the impedance spectroscopy. The inhibition efficiencies (IE_i) were calculated using the following equation:

$$\text{IE}_{\text{I}}(\%) = \left[\frac{R'_{ct} - R_{\text{ct}}}{R'_{\text{ct}}}\right] \times 100 \tag{4}$$

where R_{ct} and R'_{ct} are the charge transfer resistance values in the absence and presence of the inhibitor, respectively. The calculated impedance parameters are given in Table 3. In the case of the electrochemical impendence spectroscopy, inhibition efficiency (IE_{I}) is calculated by charge transfer resistance using the Equation 3. The double layer capacitance (C_{dl}) and the frequency at which the imaginary component of the impedance is maximum ($-Z_{\text{max}}$) are represented in the equation

$$C_{\text{dl}} = 1/\omega R_{\text{ct}} \tag{5}$$

where $\omega = 2\pi \text{f}_{\text{max}}$

From Nyquist plots in Figure 4, it is clear that the impedance diagrams in most cases do not show a perfect semicircle. This behavior can be attributed to the frequency dispersion as a result of inhomogeneities of the electrode surface.[21] These curves are dispersed in nature. Also, these curves show a single semicircle indicating the occurrence of a single charge transfer reaction. Li et al.[22], have observed this type of dispersed semicircles and reported that this kind of phenomenon is called the dispersing effect. All the Nyquist plots obtained in the present study are characterized by a single time constant. Figure 5 is the equivalent circuit used to fit the EIS data. Such an equivalent circuit was also discussed by several researchers [23–25] who obtained similar depressed semicircles with single time constant. In this equivalent circuit, R_{s} represents the solution resistance between the reference and working electrode, R_{ct} represents the charge transfer resistance corresponding to the corrosion reaction at the metal/electrolyte interface and CPE represents the constant phase element describing the interface double layer. CPE is substituted for the respective capacitor of C_{dl} in order to fit the depressed semicircles better.[26]

The impendence of CPE is defined as

$$Z_{\mathrm{CPE}} = Y_o^{-1}(\mathrm{j}\omega)^{-n} \tag{6}$$

where Y_o is the magnitude of the CPE, j is the imaginary root, ω is the angular frequency, and n is the CPE exponent which gives details about the degree of surface inhomogeneity resulting from surface roughness, inhibitor adsorption, porous layer formation, etc.[27] Depending on the value of exponent n, Z_{CPE} represents a resistance with $R = Y^{-1}$; for $n = -1$, an inductance with $C = Y$.[28] The value range of a real electrode of n is often between 0 and 1. The smaller the value of n, the rougher the electrode surface and the more serious, the corrosion of the electrode.[29]

In the present study, the surface film formed in the presence of the synergistic combination containing AS (100 ppm) and Zn^{2+} ions (50 ppm) has an R_{ct} value of 12,854 Ω cm^2, which is higher than the values of the R_{ct} obtained in the presence of the individual constitutents, i.e., 1248 Ω cm^2 for 100 ppm AS and 790 Ω cm^2 for 50 ppm Zn^{2+} ions. A larger value of R_{ct} implies the high inhibition efficiency, giving consequently a decrease in the corrosion rate. The corrosion inhibition efficiency of the synergistic combination obtained from impedance studies is 93%, which is in agreement with the efficiency obtained from the gravimetric studies. The CPE value of the metal/solution interface was 582 μF cm^{-2} in the absence of the inhibitor. A decrease in the CPE value (198 μF cm^{-2}) of the metal/solution interface is obtained in the presence of the inhibitor. The high CPE value is due to a large increase in the surface area caused by the presence of corrosion products on the carbon steel surface. Thus, for the inhibited solution a decrease in the CPE value can be explained by a decrease in the quantity of the corrosion products due to increase in the inhibition effect. Decrease in the capacitance, which can result from a decrease in the local dielectric constant and/or an increase in the thickness of the electrical double layer, strongly suggests that the inhibitor molecules adsorbed at the metal/solution interface.[30] The value of n considerably increases to 0.94 in the presence of the inhibitor system, suggesting a decrease of the inhomogeneity of the interface during the inhibition process. These results indicated that there is a formation of protective film at the metal/solution interface.[31] The impedance result of the present study also implies the synergistic action operating between AS and Zn^{2+}. This is in agreement with the inferences drawn from gravimetric studies and EIS studies.

3.5. Potentiodynamic polarization studies

Potentiodynamic polarization measurements were carried out in order to gain knowledge concerning the kinetics of the anodic and cathodic reactions. Polarization experiments were carried out potentiodynamically in control solution in the absence and presence of various inhibitor combinations and the obtained polarization curves are shown in Figure 6. The corrosion kinetic parameters derived from these curves are presented in Table 4. The corrosion potential (E_{corr}) in the case of the control is −537 mV versus SCE and the corresponding corrosion current density (i_{corr}) is 22.87 μA/cm^2. AS alone shifts the E_{corr} value to a more anodic side. In the presence of AS alone, the i_{corr} value is reduced slightly to 16.35 μA/cm^2. The shift in anodic Tafel slope (β_a) is greater than the shift in cathodic Tafel slope (β_c) in the presence of AS alone. When Zn^{2+} is considered, the corrosion potential is shifted to the cathodic side and the shift in cathodic Tafel slope is greater. Contrary to the result obtained in the case of AS, Zn^{2+} increased the rate of corrosion as implied by an

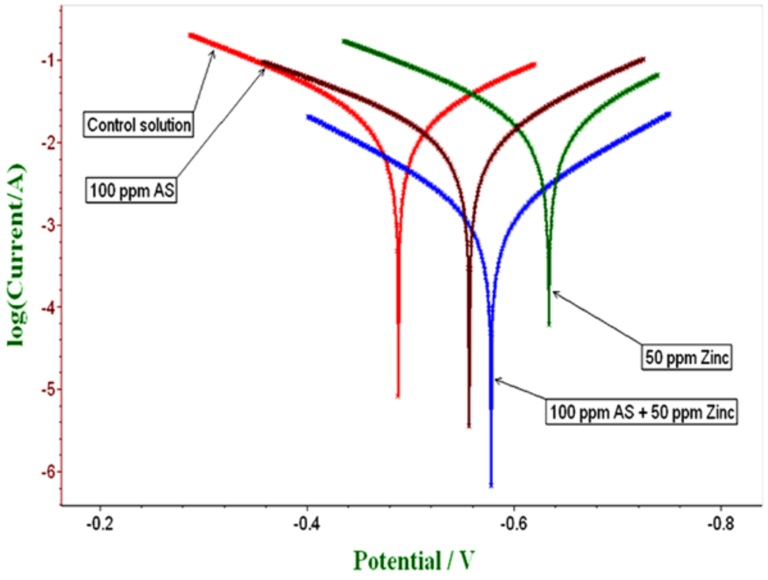

Figure 6. Potentiodynamic polarization curves for carbon steel immersed in different test solutions.

Table 4. Impedance parameters obtained from the AC impedance spectra of carbon steel immersed in the presence and absence of inhibitor system.

Concentration (ppm)					
AS	Zn^{2+}	Rct (Ωcm^2)	CPE ($\mu F/cm^2$)	*n*	IE (%)
0	0	958	582	0.78	–
0	50	781	681	0.84	–
100	0	1840	302	0.92	48
100	50	12,154	172	0.94	92

increase in corrosion current density. In the presence of Zn^{2+}, the increase in corrosion current density leads to increase in corrosion rate.[32] From the polarization curves shown in Figure 6, it is clear that the combination of AS (100 ppm) and Zn^{2+} (50 ppm) significantly decreased corrosion current density values when compared to the control and also individual components. There is a slight shift in corrosion potential to a more cathodic side, and the shift in cathodic Tafel slope is greater than the shift in anodic Tafel slope. The corrosion current density is significantly decreased from 22.87 to 2.28 $\mu A/cm^2$, corresponding to an inhibition efficiency of 90%. Thus, the synergistic mixture of 100 ppm of AS and 50 ppm of Zn^{2+} is proved to be an effective corrosion inhibitor for carbon steel. An inhibitor can be classified as an anodic or cathodic type when the change in E_{corr} value is larger than 85 mV. But in the present study, the maximum displacement is 5 mV/SCE in AS and Zn^{2+} ions system, which indicates that the inhibitor acts as a mixed-type inhibitor. On the other hand, the anodic and cathodic slope values of inhibited solution have changed with respect to uninhibited solution which also reiterates that the inhibitor is a mixed-type inhibitor. The obtained protection efficiency values are in good correlation with the values of gravimetric measurements and electrochemical impedance spectroscopy.

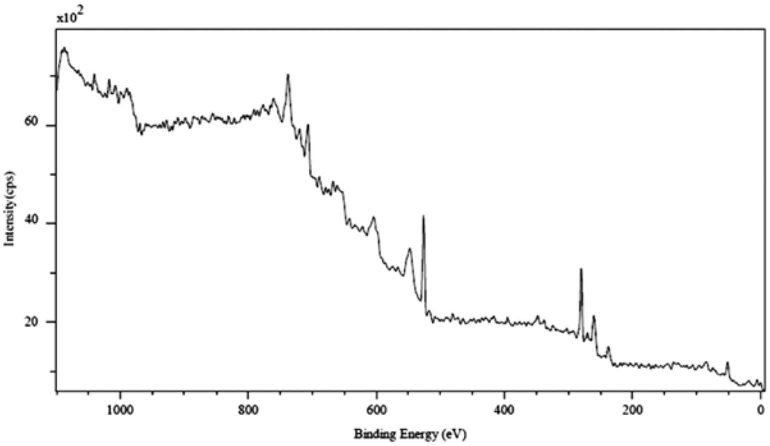

Figure 7. XPS spectrum of the general survey of the inhibited surface film (60 ppm Cl^- inos + 100 ppm AS + 50 ppm Zn^{2+}ions).

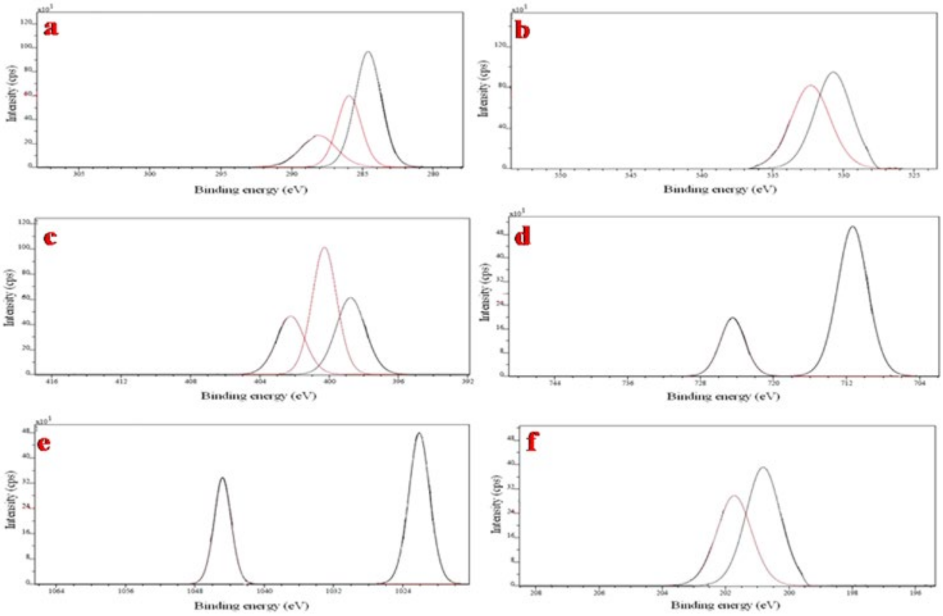

Figure 8. XPS deconvolution spectra of (a) C 1s (b) O 1s (c) N 1s (d) Fe 2p (e) Zn 2p (f) Cl 2p.

3.6. Surface examination studies

3.6.1. X-ray photoelectron spectroscopy

XPS is mostly used to determine the composition of the protective film on the metal surface.[33] XPS provides binding energy data permitting identification of elements or groups contained in the film being studied. In the XPS experiment, basically the surface of the sample is irradiated by a source of X-rays under ultra-high vacuum conditions (10–9 to 10–10 torr). The photoelectrons which result due to photoionization on the sample surface have a kinetic energy (Ek) which is expressed by Einstein's equation:

$$Ek = h\nu E_b - \phi \tag{7}$$

where $h\nu$ is the energy of the incident beam, E_b is the binding energy of the photoelectrons and Φ is the work function of the spectrometer. The excited core electrons have different kinetic energies depending on their binding energies. The identification of the given electron can be done using the binding energy of that electron. The intensity of the beam observed depends on the concentration of atoms on the surface. XPS spectra were acquired by recording the total electron current vs. kinetic energy in a computer system. Wide spectra covering the binding energy ranging from 0 to 1100 eV can be recorded for identifying the elements of the unknown sample. The binding energies of the intense lines present in the spectrum are then compared with the values reported in the literature. Even for the electrons of inner core shells, the binding energies are considerably affected by the oxidation state which changes the effective field force of the nucleus. This change in shift is called the chemical shift and it ranges from 0.1 to 10 eV. An extensive list of chemical shifts for various oxidation states for most of the elements has been compiled and is available in the literature[34]. This information on chemical states from the binding energy variation of photoelectron lines gives XPS a major advantage over other techniques.

In the present study, XPS patterns of the protective film formed on the carbon steel surface immersed in an aqueous environment of 60 ppm chloride at neutral pH in the absence and the presence of the inhibitor were recorded. The XPS pattern was interpreted with the help of the literature data for various elements exhibiting peaks at characteristic binding energy levels. The XPS patterns of the individual elements for the above system relating to chlorine, carbon, oxygen, and iron are not shown in figures. The Cl $2p_{1/2}$ peak appeared at 201.11 eV. The peaks at 287.5 and 290.4 eV correspond to C 1s which appeared even in the absence of any inhibitor. These carbon peaks are due to residual carbon from oil vapors of the diffusion pump while recording the XPS spectrum with the instrument. Similar carbon peaks are reported in the literature in the XPS spectrum for the same reason. These peaks appeared due to surface contamination.[35–38] The presence of adsorbed water molecules is reported to exhibit the peak at 533.2 eV.[39–41] However, there is a formation of a brown film consisting of oxides/hydroxides of iron on the iron surface. Therefore, the broad peak due to O 1s at 533.4 eV in the present study can be interpreted to occur due to the presence of not only the adsorbed H_2O molecules but also oxides/hydroxides of iron. This interpretation can be seen along with the interpretation of the iron peak discussed below. Two peaks appeared for iron, one at 713.9 eV and the other at 727.1 eV. The former peak corresponds to Fe $2p_{3/2}$ and the latter peak corresponds to Fe $2p_{1/2}$. The shifts in both the peaks from the corresponding binding energy values of elemental iron are quite significant. These shifts are due to the formation of iron oxides/hydroxides on the carbon steel surface.

The XPS pattern of the protective surface film of carbon steel specimen immersed in 60 ppm chloride ions, 100 ppm AS, and 50 ppm Zn^{2+} for a period of 7 days is also given in Figure 7. The XPS deconvoluted spectra of the individual elements of carbon, oxygen, nitrogen, iron, zinc, and chlorine are given in Figure 8(a)–(f).

The C1s spectrum has three peaks; one is the more intense peak at 284.62 eV and other two are less intense peaks at 285.94 and 288.13 (Figure 8(a)). The shift from 285 eV, which is characteristic for elemental carbon. The presence of multiple peaks in the C 1s spectrum in the case of the inhibitor can be attributed to various carbon environments present in the AS. The intensity of the C 1s peaks in the presence of the inhibitor is about twice as that of the peak in the case of control. This interpretation can be supported from studies reported in the literature[24,36,37,42]. Labjar et al. [43] had studied ATMP-treated carbon steel surface by XPS spectra of C 1s which showed three peaks and concluded that a binding energy of 284.7 eV was attributable to the C–H, the second peak may be assigned to the C–N bond in the ATMP ring at 286.7 eV, the last peak may be ascribed to the C–O or C–P in the ATMP ring at 288.9 eV.

In the O 1s spectrum, the peaks were observed at 530.75 and 532.30 eV (Figure 8(b)). The O 1s peak observed at 530.75 eV is due to O^{2-}, the presence of O^{2-} in the surface film may be in the form of oxides and hydroxides of Fe(III).[37,44]. The peak at 532.30 eV may be due to the coordination of oxygen to the metal ion resulting in complex formation. Similar findings were reported by Felhosi et al. [39] and Karman et al. [40] The O 1s peak of high intensity was observed at 530.75 eV. It may be interpreted as follows. The XPS of the surface film shows the presence of carbon, iron, and zinc. It means that AS is present on the surface, zinc is present as Zn^{2+} and the interpretation given in the case of Fe 2p indicates the presence of Fe_2O_3, Fe_3O_4, and FeOOH. Hence, the O 1s peak observed in the inhibited surface films can be ascribed to the presence of $Zn(OH)_2$, Fe_2O_3, Fe_3O_4, FeOOH and/or Fe $(OH)_2$ and oxygen of AS in the inhibited film.[36,44,45] Ochoa et al. [42] interpreted that the O 1s peak at 533.2 eV corresponds to O=C group which is bonded to iron surface. It may also be due to the presence of the adsorbed H_2O molecules.

Figure 8(c) shows the N 1s peaks in the XPS spectrum of the surface film, one at 398.79 eV and another at 402.23 eV. This peak is shifted from the characteristic elemental binding energy value of 398.0 eV for nitrogen.[46] This shift may be attributed to the presence of AS molecules in the surface film in the form of a complex with Fe(III) and Zn(II).[47] Meneguzzi et al. [48] reported that the peak at 399.9 eV could be attributed to the neutral imine (–N=) and amine (–N–H) nitrogen atoms. Li et al. [49] reported that the peaks at 401.3 and 402.8 eV can be assigned to protonated amine. Therefore, the peak that appeared at 402.23 eV in the present study may be due to absorbed and complexes AS through nitrogen.

The XPS spectrum of Fe 2p in the case of the inhibitor formulation is shown in Figure 8(d). It shows two peaks, one with a lower binding energy value (711.38 eV) corresponding to Fe $2p_{3/2}$ electron and the other one with a higher binding energy value (724.51 eV) corresponding to Fe $2p_{1/2}$ electron. The peak due to Fe $2p_{3/2}$ is interpreted for the determination of the chemical state of iron in the surface film. The Fe $2p_{3/2}$ peak at 711.38 eV has shifted from 707 eV for elemental iron.[34] The Fe $2p_{1/2}$ peak has also shifted from 720 to 724.51 eV. Similar shifts were also observed by Felhosi et al. and Karman et al. [39,40] Such a large shift suggests that iron is present in Fe^{3+} state in the surface film. This shift may be ascribed to the presence of iron in the Fe^{3+} state in the form of $Fe(OH)_3$, FeOOH, γ-Fe_2O_3, and [Fe(III)–AS] complex.[44,46,50] The binding energy of Fe^{2+} state in iron oxides is reported to be around 708.5 eV.[41] The absence of any peak in this region in the present study also supports that iron does not exist in Fe^{2+}, but in Fe^{3+} state in the surface film. Paszternak et al., reported that the Fe $2p_{3/2}$ and Fe $2p_{1/2}$ peaks were decomposed into two main compounds; the metallic iron (Fe $2p_{3/2}$ at 707 and Fe $2p_{1/2}$ at 719.5 eV) and the mixture of Fe^{3+} and Fe^{2+} (Fe $2p_{3/2}$ at 711 and Fe $2p_{1/2}$ at 724 eV) and confirmed the dominant chemical state in the oxide is the Fe^{3+} in their alkyl phosphonated film on iron surface.[51]

Figure 8(e) shows the Zn 2p spectrum, the peaks that were observed at 1021.4 and 1044.84 eV. The binding energy of Zn $2p_{3/2}$ is shifted from 1021.4 eV for elemental zinc to 1022 eV and the binding energy of Zn $2p_{1/2}$ is shifted from 1044 to 1044.84 eV. Aramaki reported the Zn peak at 1022.7 and 1021.7 eV in the spectra of Zn $2p_{3/2}$ and concluded that the surface layer consisted of $Zn(OH)_2$ at the outer layer and ZnO at the inner part mostly.[52] Aramaki [53] studied the effect of sodium phosphate on protective films on a zinc electrode by XPS where the Zn peak of $Zn(OH)_2$, appeared at 1022.8 eV. In the present study also Zn 2p3/2 peak appeared at 1022.13 eV, which confirms the formation of $Zn(OH)_2$.[52] This peak may also be due to the involvement of Zn(II) in complex with AS.

Along with the elements discussed above, the deconvoluted XPS spectrum in the case of chlorine in inhibited surface is shown in Figure 8(f). A peak at 199.09 eV appeared for chlorine whereas in the case of control, a low-intensity chlorine peak is seen at 200.80 eV. This indicates the decreased adsorption of chlorine leading to higher resistance against localized corrosion. The present study also shows that the presence of small amounts of chlorine and subsequent adsorption of aggressive ions on metal surfaces is decreased, thereby allowing inhibitor molecules to cover the entire surface and protecting the metal.

After consolidating all the inferences drawn from the XPS of individual elements (Fe, N, C, O, Zn and Cl) present in surface films, it is suggested that the surface film consists of mainly [Zn(II)–AS] complex, $Zn(OH)_2$, and small amounts of oxides / hydroxides of Fe(III) in the case of the inhibitor system. The complex may be chemisorbed on the metal surface and got attached to the Fe(III) ions.[54]

3.6.2. Fourier transform infrared spectroscopy

FTIR spectra have been used to analyze the protective film formed on the metal surface. The FTIR spectrum of KBr pellet of pure AS is shown in Figure 9(a). The C=O stretching frequency of carboxyl group appears at 1689 cm^{-1}. The C–N stretching frequency appears at 1139 cm^{-1}. The N–H stretching frequency of the amine group appears at 3139 cm^{-1}.[55] The FTIR spectrum of AS with Zn^{2+} is shown in the Figure 9(b). The C=O stretching frequency has shifted from 1689 to 1618 cm^{-1}. The C–N stretching frequency has shifted from 1139 to 1018 cm^{-1}. The N–H stretching frequency has shifted from 3139 to 3252 cm^{-1}. The peak at 1401 cm^{-1} indicates the presence of $Zn(OH)_2$ on the metal surface film.[56]

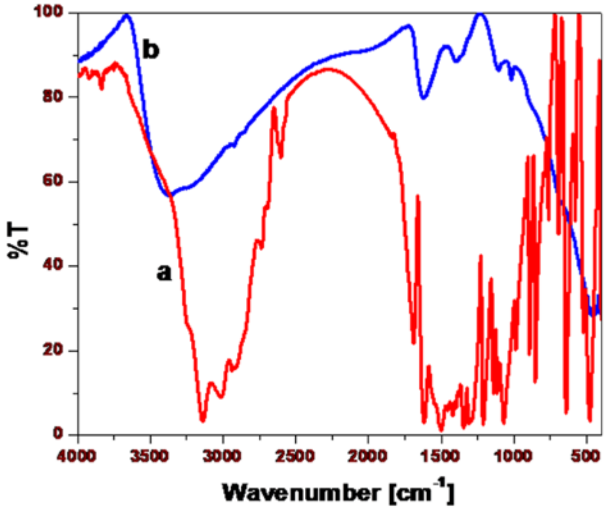

Figure 9. FTIR spectra of (a) pure AS and (b) surface film.

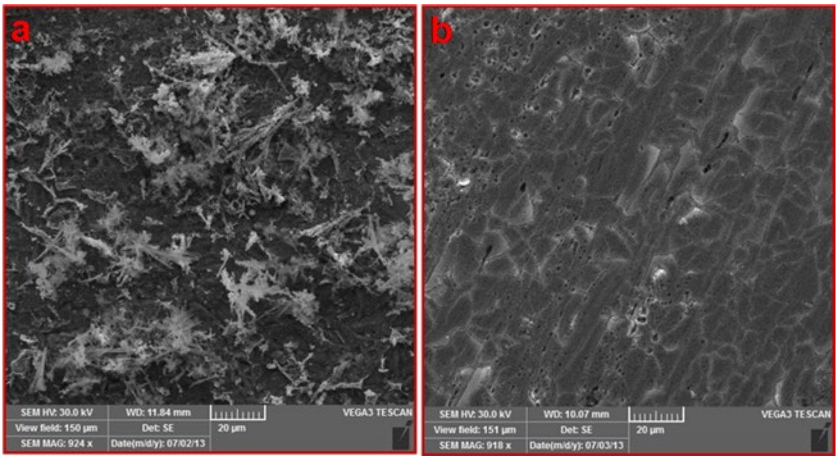

Figure 10. SEM images of carbon steel immersed in (a) control solution and (b) presence of inhibitor system.

The broad band of the OH stretching and bending mode of water or hydroxides within the protective film appeared at 3389 cm^{-1}. There are many weak bands in the region between 1200 and 400 cm^{-1} and a peak of high intensity appeared at 437 cm^{-1} implying the presence of ferric and ferrous oxides and hydroxide in the protective film.[53,57] The FTIR spectra suggests that what the protective film may consist of [Fe(II)/Zn(II)–AS], $Zn(OH)_2$ and small amounts oxides and hydroxides of iron.

3.6.3. Scanning electron microscopy

The surface images of the carbon steel were examined in the presence and absence of inhibitors (AS–Zn^{2+}). The SEM micrograph of carbon steel after exposure for 7 days in a solution without inhibitor is shown in Figure 10(a). The image has several pits and cracks. The pits that appear in the image show that the metal was corroded severely and contains iron oxides as corrosion product. Several white patches seen in the image show the presence of some other form of corrosion products also.

The surface of carbon steel after the immersion of 7 days in an aqueous solution containing 60 ppm Cl$^-$, 50 ppm Zn^{2+} and 100 ppm AS is shown in Figure 10(b). It can be seen that the adsorbed protective film is formed and consequently retards the dissolution of metal. It is important to know that when AS was present in the solution, the surface morphology of the carbon steel is quite different from the previous one and the AS forms some kind of complex with iron on the substrate. It may be concluded the SEM micrograph reveals that the protective surface film formed by the inhibitor system exhibits good inhibitive properties for carbon steel in aqueous environment.

3.6.4. Atomic force microscopy

AFM is a powerful method to examine the surface morphology at nano- to micro-scale and has become a new choice to study the influence of inhibitors on the generation and the progress of the corrosion at the metal–solution interface.[58] The topography of the surfaces recorded in 2D and 3D images was examined and surface roughness, RMS, and mean roughness factor (R_a) were determined from the respective images. Figure 11(a)

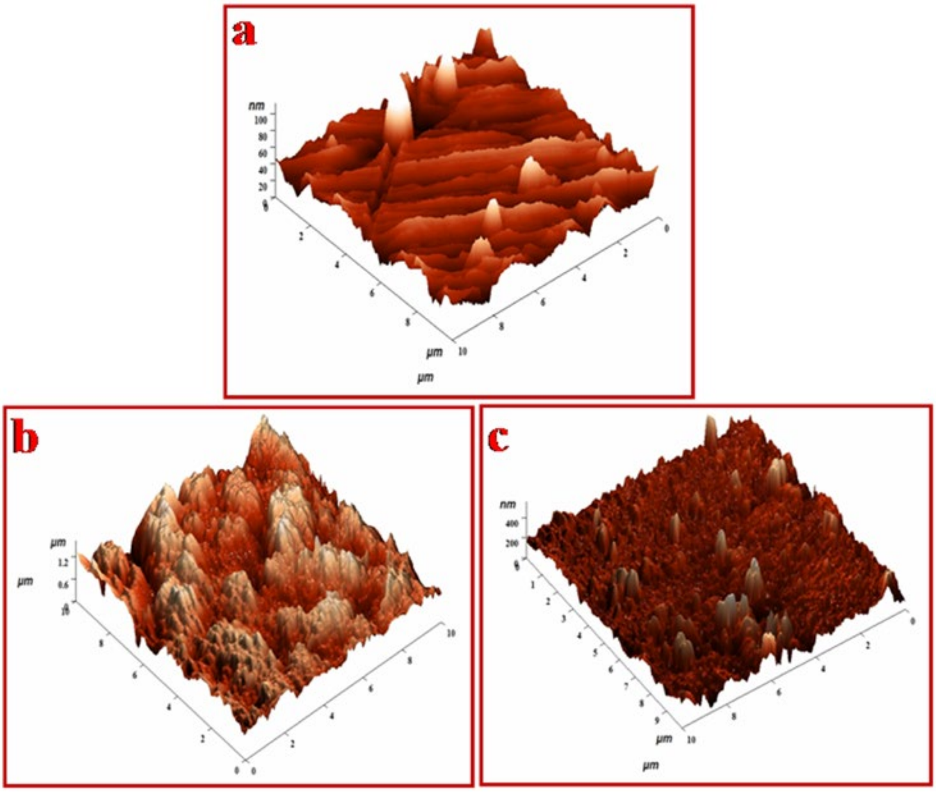

Figure 11. AFM topographical images of carbon steel surface after immersion in control in the absence and presence of the inhibitor: (a) polished carbon steel, (b) control solution, and (c) inhibitor system.

shows the AFM image of the polished metal surface, with an R_a value of 6.83, RMS value of 9.47 nm, and ΔZ value of 56.65 nm when compared with other thin film coated surface values indicating the absence of iron oxides on the smooth surface. A severely corroded surface morphology (Figure 11(b)) is observed after immersion in the control in the absence of the inhibitor, with an increased R_a value of 183.84 nm, RMS value of 230.36 nm, and ΔZ value of 826.53 nm, indicating the formation of iron oxides. The RMS value is found to be 230.36 nm, which clearly indicates the high roughness of the corroded surface. The microstructure of the surface shows several smaller and larger corrosion product deposits. However, Figure 11(c) shows that the carbon steel immersed in inhibitor, 100 ppm AS, and 50 ppm Zn^{2+} showed a decreased R_a value of 38.85 nm, RMS value of 52.45 nm, and ΔZ value of 268.76 nm, which indicates the formation of a protective film on the metal surface.[59]

3.7. Mechanism of corrosion protection

The following plausible mechanism of corrosion inhibition can be proposed,

Carbon steel immersed in an aqueous solution undergoes initial corrosion to form Fe^{2+} ions at the anodic sites.

$$\mathrm{Fe} \rightarrow \mathrm{Fe}^{2+} + 2\mathrm{e}^{-} \tag{7}$$

Fe^{2+} further undergoes oxidation in the presence of oxygen available in the aqueous solution.

$$Fe^{2+} \xrightarrow{[O_2]} Fe^{3+} + e^{-} \tag{8}$$

The corresponding reduction reaction at cathodic sites

$$O_2 + 2H_2O + 4e^{-} \rightarrow 4OH^{-} \tag{9}$$

Fe^{2+} ions formed at anodic sites and OH^- ions formed at cathodic sites combine to form $Fe(OH)_2$. Apart from $Fe(OH)_2$, there is formation of other oxides and hydroxides like FeOOH, γ-Fe_2O_3, etc., on the carbon steel surface before the formation of the protective film.

When AS and Zn^{2+} ions are added to the aqueous solution, AS reacts with Zn^{2+} to form a complex [Zn(II)–AS]. This complex diffuses into the metal surface and reacts with Fe^{2+}/ Fe^{3+} ions available at the anodic sites to form [Fe(II)/Fe(III)/Zn(II)–AS] complex which covers the anodic sites and controls the corresponding reaction at anodic sites.

$$[Zn(II) - AS] + Fe^{2+}/Fe^{3+} \rightarrow [Fe(II)/\,Fe(III)/Zn\,(II) - AS] \tag{10}$$

Free Zn^{2+} ions available in the bulk of the solution diffuse into the metal surface and react with OH^- ions produced at the cathodic sites to form a precipitate of $Zn(OH)_2$. This precipitate gets deposited on the cathodic sites and controls the cathodic reaction.

$$Zn^{2+} + 2\,OH^{-} \rightarrow Zn(OH)_2 \tag{11}$$

Thus, AS and Zn^{2+} play a very important role in the synergistic effect in controlling corrosion through the formation of a protective film on the carbon steel surface. Similar reports of complex formation have been noted in the literature[44,56,59].

4. Conclusions

Based on the above results, the following conclusion can be drawn:

(1) All the measurements showed that the AS–Zn^{2+} system has excellent inhibition properties for the corrosion of carbon steel in an aqueous solution. The gravimetric measurements showed that the inhibition efficiency increases on increasing the concentration of AS.
(2) The inhibitor system 100 ppm AS and 50 ppm Zn^{2+} is effective and has 96% IE.
(3) This inhibitor formulation is effective in the pH range of 5.0–7.0 and also at pH 11.0.
(4) Potentiodynamic polarization measurements showed that the AS acts as a mixed-type inhibitor predominantly of cathodic nature. EIS measurements also indicate that the inhibitor concentration increases, with an increase in the charge transfer resistance and showed that the inhibitive property depends on the adsorption of the molecules on the metal surface.
(5) The protective film may consist of [Fe(III)/Fe(II)/Zn(II)–AS] complex, $Zn(OH)_2$, hydroxides, and oxides of iron.
(6) This multi-component formulation consisting of AS and Zn^{2+} can be used as a potential inhibitor to prevent the corrosion of carbon steel in neutral aqueous solution.

Acknowledgments

One of the authors, M. Prabakaran, is thankful to the UGC for the fellowship under Research Fellowship in Sciences for Meritorious Students. The authors thank the Co-ordinator, UGC-SAP, Department of Chemistry, GRI for his help and also thank the authorities of Gandhigram Rural Institute for the encouragement.

Disclosure statement

No potential conflict of interest was reported by the authors.

References

[1] Benabdellah M, Dafali A, Hammouti B, et al. The role of phosphonate derivatives on the corrosion inhibition of steel in HCL media. Chem. Eng. Commun. 2007;194:1328–1341.
[2] Khaled KF, Hackerman N. Investigation of the inhibitive effect of ortho-substituted anilines on corrosion of iron in 1 M HCl solutions. Electrochim. Acta. 2003;48:2715–2723.
[3] Fouda AS, Ellithy AS. Inhibition effect of 4-phenylthiazole derivatives on corrosion of 304L stainless steel in HCl solution. Corros. Sci. 2009;51:868–875.
[4] El-Taib Heakal F, Fouda AS, Radwan MS. Inhibitive effect of some thiadiazole derivatives on C-steel corrosion in neutral sodium chloride solution. Electrochim. Acta.2011;125:26–36.
[5] Fouda AS, Abdallah M, Ahmed IS, et al. Corrosion inhibition of aluminum in 1 M H_3PO_4 solutions by ethanolamines. Arabian J. Chem. 2012;5:297–307.
[6] Chetouani A, Aouniti A, Hammouti B, et al. Corrosion inhibitors for iron in hydrochloride acid solution by newly synthesised pyridazine derivatives. Corros. Sci. 2003;45:1675–1684.
[7] Bouklah M, Hammouti B, Lagrenee M, et al. Thermodynamic properties of 2,5-bis (4-methoxyphenyl)-1,3,4-oxadiazole as a corrosion inhibitor for mild steel in normal sulfuric acid medium. Corros. Sci. 2006;48:2831–2842.
[8] Abdallah M, Helal EA, Fouda AS. Aminopyrimidine derivatives as inhibitors for corrosion of 1018 carbon steel in nitric acid solution. Corros. Sci. 2006;48:1639–1654.
[9] Chetouani A, Hammouti B, Aouniti A, et al. New synthesised pyridazine derivatives as effective inhibitors for the corrosion of pure iron in HCl medium. Prog. Org. Coat. 2002;45:373–378.
[10] Baral A, Engelken RD. Chromium-based regulations and greening in metal finishing industries in the USA. Environ. Sci. Policy. 2002;5:121–133.
[11] Gaidis JM. Chemistry of corrosion inhibitors. Cem. Concr. Compos. 2004;26:181–189.
[12] Stupnisek-Lisac E, Loncaric Bozic A, Cafuk I. Low-toxicity copper corrosion inhibitors. Corrosion. 1998;54:713–720.
[13] Zerfaoui M, Oudda H, Hammouti B, et al. Inhibition of corrosion of iron in citric acid media by aminoacids. Prog. Org. Coat. 2004;51:134–138.
[14] Yadav M, Kumar S, Gope L. Experimental and theoretical study on amino acid derivatives as eco-friendly corrosion inhibitor on mild steel in hydrochloric acid solution. J. Adhes. Sci. Technol. 2014;28:1072–1089.
[15] Aouinti A, Hammouti B, Brighli M, et al. L-methionine methyl ester hydrochloride as a corrosion inhibitor of iron in acid chloride solution. Corrosion. 1995;51:411–416.
[16] Aksut AA, Bilgic S. The effect of amino acids on the corrosion of nickel in H_2SO_4. Corros. Sci. 1982;33:379–387.
[17] Bouzidi D, Kertit S, Hammouti B, et al. Some aminoacids as non toxic inhibitors for the corrosion of iron in 0.5 M H_2SO_4. J. Electrochem. Soc. 1997;46:23–30.
[18] Ranjana, Banerjee R, Nandhi MM. Inhibition effect of amino acid derivatives on the corrosion of brass in 0.6 M aqueous sodium chloride solution. Ind. J. Chem. Technol. 2010;17:176–180.
[19] Hasanov R, Sadıkoglu M, Bilgic S. Electrochemical and quantum chemical studies of some Schiff bases on the corrosion of steel in H_2SO_4 solution. Appl. Surf. Sci. 2007;253:3913–3921.

[20] Sherif El-Sayed M. Effects of 5-(3-aminophenyl)-tetrazole on the inhibition of unalloyed iron corrosion in aerated 3.5% sodium chloride solutions as a corrosion inhibitor. Mater. Chem. Phys. 2011;129:961–967

[21] Juttner K. Electrochemical impedance spectroscopy (EIS) of corrosion processes on inhomogeneous surfaces. Electrochim. Acta. 1990;35:1501–1508.

[22] Li SL, Ma HY, Lei SB, et al. Inhibition of copper corrosion with schiff base derived from 3-methoxysalicylaldehyde and O-phenyldiamine in chloride media. Corrosion. 1998;54:947–954.

[23] Alagta A, Felhosi I, Teleghi J, et al. Effect of metal ions on corrosion inhibition of pimeloyl-1,5-di-hydroxamic acid for steel in neutral solution. Corros. Sci. 2007;49:2754–2766.

[24] Gunasekaran G, Chauhan LR. Eco friendly inhibitor for corrosion inhibition of mild steel in phosphoric acid medium. Electrochim. Acta. 2004;49:4387–4395.

[25] Morad MS. An electrochemical study on the inhibiting action of some organic phosphonium compounds on the corrosion of mild steel in aerated acid solutions. Corros. Sci. 2000;42:1307–1326.

[26] Mansfeld F, Kendig MW, Lorenz WJ. Corrosion inhibition in neutral, aerated media. J. Electrochem. Soc. 1985;132:290–296.

[27] Pavithra MK, Venkatesha TV, Vathsala K, et al. Synergisitic effect of halide ions on improving corrosion inhibition behavior of benzisothiozloe-3-piperizine hydrochloride on mild steel in 0.5 M H_2SO_4 medium. Corros. Sci. 2010;52:3811–3819.

[28] Ross Macdonald J. Impedance spectroscopy and its use in analyzing the steady-state AC response of solid and liquid electrolytes. Electrochim. Acta. 1987;223:25–50.

[29] Khaled KF, Hackerman N. Ortho-substituted anilines to inhibit copper corrosion in aerated 0.5 M hydrochloric acid. Electrochim. Acta. 2004;49:485–495.

[30] Zarrok H, Oudda H, El Midaoui A, et al. Some new bipyrazole derivatives as corrosion inhibitors for C38 steel in acidic medium. Res. Chem. Intermed. 2012;38:2051–2063.

[31] Bentiss F, Traisnel M, Lagrenee M. The substituted 1,3,4-oxadiazoles: a new class of corrosion inhibitors of mild steel in acidic media. Corros. Sci. 2000;42:127–146.

[32] Rajendran S, AppaRao BV, Palaniswamy N. Investigation of the inhibiting effect of ethyl phosphonic acid-Zn^{2+} system. Bull. Electrochem. 2001;17:171–174.

[33] Chopra DR, Chowrasia AR. X-ray photoelectron spectroscopy. In: Settle FA, editor. Handbook of instrumental techniques for analytical chemistry. Upper Saddle River, NJ: Prentice Hall PTR; 1997.

[34] Moulder JF, Stickle WF, Sobol PE, et al. Handbook of X-ray photoelectron spectroscopy: a reference book of standard spectra for identification and interpretation of XPS data. Eden Prairie, MN: Physical Electronics; 1995.

[35] Kadirgan F, Suzer S. Electrochemical and XPS studies of corrosion behaviour of a low carbon steel in the presence of FT2000 inhibitor. J. Electron Spectrosc. Relat. Phenom. 2001;114–116:597–601.

[36] Royd RD, Verron J, Hall KE, et al. The cleanability of stainless steel as determined by X-ray photoelectron spectroscopy. Appl. Surf. Sci. 2001;17:135–143.

[37] Suji NT, Nozawa K, Aramaki K. Ultrathin protective films prepared by modification of an N, N-dimethylalkylamine monolayer with chlorosilanes for preventing corrosion of iron. Corros. Sci. 2000;42:1523–1538.

[38] Welle A, Liao JD, Kaiser K, et al. Interactions of *N,N′*-dimethylaminoethanol with steel surfaces in alkaline and chlorine containing solutions. Appl. Surf. Sci. 1997;119:185–198.

[39] Felhosi I, Keresztes Zs, Karman FH. Effects of bivalent cations on corrosion inhibition of steel by 1-hydroxyethane-1,1-diphosphonic acid. J. Electrochem. Soc. 1999;146:961–969.

[40] Karman FH, Felhosi I, Kalman E, et al. The role of oxide layer formation during corrosion inhibition of mild steel in neutral aqueous media. Electrochim. Acta. 1998;43:69–75.

[41] Asami K, Hashimoto K, Shimodaira S. X-ray photoelectron spectrum of Fe^{2+} state in iron oxides. Corros. Sci. 1976;16:35–45.

[42] Ochoa N, Baril G, Moran F, et al. Study of the properties of a multi-component inhibitor used for water treatment in cooling circuits. J. Appl. Electrochem. 2002;32:497–504.

[43] Labjar N, EI Hajjaji S, Lebrini M, et al. Enhanced corrosion resistance properties of carbon steel in hydrochloric acid medium by aminotris-(methylenephosphonic): surfacecharacterizations. J. Mater. Environ. Sci. 2011;2:309–318.

[44] Pech-Canul MA, Bartolo-Perez P. Inhibition effects of N-phosphono-methyl-glycine/Zn^{2+} mixtures on corrosion of steel in neutral chloride solutions. Surf. Coat. Technol. 2004;184: 133–140.

[45] Babic-Samardzija K, Lupu K, Hackerman N, et al. Inhibitive properties and surface morphology of a group of heterocyclic diazoles as inhibitors for acidic iron corrosion. Langmuir. 2005;21:12187–12196.

[46] Kalman E, Karman FH, Cserny I, et al. The effect of calcium ions on the adsorption of phosphonic acid: a comparative investigation with emphasis on surface analytical methods. Electrochim. Acta. 1994;39:1179–1182.

[47] El Azhar M, Traisnel M, Mernari B, et al. Electrochemical and XPS studies of 2,5-bis (n-pyridyl)-1,3,4-thiadiazoles adsorption on mild steel in perchloric acid solution. Appl. Surf. Sci. 2002;185:197–205.

[48] Meneguzzi A, Ferreira CA, Pham MC, et al. Electrochemical synthesis and characterization of poly(5-amino-1-naphthol) on mild steel electrodes for corrosion protection. Electrochim. Acta. 1999;44:2149–2156.

[49] Li P, Lin JY, Tan KL, et al. Electrochemical impedance and X-ray photoelectron spectroscopic studies of the inhibition of mild steel corrosion in acids by cyclohexylamine. Electrochim. Acta. 1997;42:605–615.

[50] McIntyre NS, Zetaruk DG. X-ray photoelectron spectroscopic studies of iron oxides. Anal. Chem. 1977;49:1521–1529.

[51] Paszternak A, Felhosi I, Paszti Z, et al. Surface analytical characterization of passive iron surface modified by alkyl-phosphonic acid layers. Electrochim. Acta. 2010;55:804–812.

[52] Aramaki K. Effects of organic inhibitors on corrosion of zinc in an aerated 0.5 M NaCl solution. Corros. Sci. 2001;43:1985–2000.

[53] Aramaki K. Preparation of self-healing protective films on a zinc electrode treated in a cerium(III) nitrate solution and modified with sodium phosphate and cerium(III) nitrate. Corros. Sci. 2004;46:1565–1579.

[54] Ashok Kumar SL, Gopiraman M, Kumar MS. 2-Acetylpyridine-*N*(4)-morpholine thiosemicarbazone (HAcpMTSc) as a corrosion inhibitor on mild steel in HCl. Ind. Eng. Chem. Res. 2011;50:7824–7832.

[55] Nakamoto K. Infrared and Raman spectra of inorganic and co-ordination compounds. 4th ed. New York (NY): Wiley; 1986.

[56] Sekine I, Hirakawa Y. Effect of 1-hydroxyethylidene-1, 1-diphosphonic acid on the corrosion of ss 41 steel in 0.3% sodium chloride solution. Corrosion. 1986;42:272–277.

[57] Nakayama N. Inhibitory effects of nitrilotris(methylenephosphonic acid) on cathodic reactions of steels in saturated $Ca(OH)_2$ solutions. Corros. Sci. 2000;42:1897–1920.

[58] Satapathy AK, Gunasekaran G, Sahoo SC, et al. Corrosion inhibition by *Justicia gendarussa* plant extract in hydrochloric acid solution. Corros. Sci. 2009;51:2848–2856.

[59] Srinivasa Rao S, Appa Rao BV, Roopas Kiran S, et al. Lactobionic Acid as a new synergist in combination with phosphonate–Zn(II) system for the corrosion inhibition of carbon steel. J. Mat. Sci. Technol. 2014;30:77–89.